Fusion Engineering and Design 191 (2023) 113545

Contents lists available at ScienceDirect

Fusion Engineering and Design

journal homepage: www.elsevier.com/locate/fusengdes

Development of the diagnostic tools for the COMPASS-U tokamak and plans for the first plasma

Vladimir Weinzettl [a,*], Petra Bilkova [a], Ivan Duran [a], Martin Hron [a], Radomir Panek [a], Tomas Markovic [a,b], Mykyta Varavin [a,c], Jordan Cavalier [a], Karel Kovarik [a], André Torres [a,d], Ekaterina Matveeva [a,b], Petr Böhm [a], Ondrej Ficker [a,c], Jan Horacek [a], Jaroslav Cerovsky [a,c], Jaromir Zajac [a], Jiri Adamek [a], Miglena Dimitrova [a], Martin Imrisek [a,b], Miroslav Sos [a,c], Eva Tomesova [a], Petr Vondracek [a], Katarzyna Mikszuta-Michalik [a,e], Jakub Svoboda [a,c], Diana Naydenkova [a], Klara Bogar [a], Jakub Caloud [a,c], Vladislav Ivanov [a,c], Samuel Lukes [c], Ales Podolnik [a], Ondrej Bogar [a], Slavomir Entler [a], Ales Havranek [a], Josef Preinhaelter [a], Fabien Jaulmes [a], Renaud Dejarnac [a], Vojtech Balner [a], Viktor Veselovsky [a], Pavel Belina [a], Miroslav Kral [a], Jonathan Gerardin [a], Jiri Vlcek [a], Momtaz Tadros [a], Pavel Turjanica [f], Vladimir Kindl [f], Jan Reboun [f], William Rowan [g], Saeid Houshmandyar [h], Marek Scholz [i], Jakub Bielecki [i], Dariusz Makowski [j], Maryna Chernyshova [e], Dario Cipciar [k]

[a] Institute of Plasma Physics of the Czech Academy of Sciences, Prague, Czechia
[b] Charles University, Faculty of Mathematics and Physics, Prague, Czechia
[c] Faculty of Nuclear Sciences and Physical Engineering, Czech Technical University in Prague, Prague, Czechia
[d] Instituto de Plasmas e Fusão Nuclear, Instituto Superior Técnico, Universidade de Lisboa, Lisbon, Portugal
[e] Institute of Plasma Physics and Laser Microfusion, Warsaw, Poland
[f] Faculty of Electrical Engineering, University of West Bohemia in Pilsen, Pilsen, Czechia
[g] Institute for Fusion Studies, The University of Texas at Austin, Austin, United States
[h] General Atomics, San Diego, United States
[i] Institute of Nuclear Physics Polish Academy of Sciences, PL-31342 Krakow, Poland
[j] Lodz University of Technology, Department of Microelectronics and Computer Science, Lodz, Poland
[k] Max-Planck-Institut für Plasmaphysik, Greifswald, Germany

ARTICLE INFO

Keywords:
Plasma diagnostics
Tokamak
COMPASS-U
Diagnostic design

ABSTRACT

The COMPASS-U tokamak ($R = 0.894$ m, $a = 0.27$ m, $B_t = 5$ T, $I_p = 2$ MA) is a new medium-size device with fully metallic plasma facing components, currently under construction at the Institute of Plasma Physics of the Czech Academy of Sciences in Prague. It features a unique combination of parameters, such as a high temperature of the tokamak walls up to 500 °C allowing a high recycling regime, a high magnetic field connected with a high plasma density above $10^{20}\ m^{-3}$ and with a high heat flux (perpendicular to divertor targets) density at the outer strike-point up to 90 MW/m^2 in attached conditions. These parameters of the device pose strict constraints and requirements on the design of individual diagnostic systems. Strategy and present status of the development of the diagnostic systems for COMPASS-U are provided. Plans for a diagnostic set for the first plasma are reviewed. The review of the diagnostics systems involves the high-temperature compatible slow (up to 20 kHz) and fast (up to several MHz) inductive and non-inductive magnetic sensors (including Thick Printed Copper coils and Hall sensors), the sub-millimetre interferometer with an unambiguous channel, Electron Cyclotron Emission, the interlock and overview cameras, high resolution Thomson scattering, radiation diagnostics (neutron diagnostics, soft and hard X-ray diagnostics, bolometers, impurity monitors, effective ion charge), probe diagnostics (including rail probes) and manipulators.

* Corresponding author.
E-mail address: weinzettl@ipp.cas.cz (V. Weinzettl).

https://doi.org/10.1016/j.fusengdes.2023.113545
Received 11 October 2022; Received in revised form 13 January 2023; Accepted 4 February 2023
Available online 16 February 2023

1. Introduction

The project for the design and construction of the high magnetic field COMPASS-U tokamak [1] was initiated at the Institute of Plasma Physics of the Czech Academy of Sciences in Prague in 2018. The Final Design Review of the main tokamak systems [2] was successfully passed in 2021 and the procurement of these systems is now in progress. COMPASS-U features a unique combination of parameters, such as the possibility to heat the tokamak walls up to 500 °C allowing a high recycling regime, a high magnetic field connected with a high plasma density above 10^{20} m^{-3} and with a high heat flux (perpendicular to divertor targets) density at the outer strike-point up to 90 MW/m^2 in attached conditions, caused by an expected strong auxiliary heating of about several MW of Neutral Beam Injection (NBI) and Electron Cyclotron Resonant Heating (ECRH), and the proposed future use of the liquid metal divertor. These parameters of the device pose strict constraints and requirements on the design of individual diagnostic systems which were discussed in [3].

In order to be able to explore the Scrape-Off-Layer (SOL) behaviour in the full wall recycling regime relevant to DEMO operation as well as to test liquid metal concepts for the divertor region of COMPASS-U [1], cutting-edge technologies compatible with high temperature of vacuum vessel (VV) components have to be chosen. For diagnostics, we are mainly inspired by three devices, designed with high-temperature compatibility in mind: TEXTOR, DIII-D and KSTAR. The vacuum vessel of TEXTOR was heatable up to 400 °C and the liner itself up to 500 - 600 °C [4], thus, magnetic sensors had to be built from heat resistant materials compatible with ultra-high-vacuum [5]. Recycling studies were done at temperatures of 150 and 350 °C [6]. DIII-D was designed allowing baking of the vacuum vessel up to 350 - 400 °C [7], having correspondingly temperature-resistant magnetic diagnostics [8]. Amongst devices built in this century, KSTAR counts with the vacuum vessel baking above 250 °C [9], having the wall interspace filled by hot nitrogen at 350 °C [10]. However, in contrast to the above-mentioned devices, the COMPASS-U diagnostics should not only withstand the elevated temperatures but, for a majority of them, it has to be also operational even in the temperature range of 300 – 500 °C. Some of the main approaches and key results along the path toward design and development of such diagnostic systems for COMPASS-U are summarised in this paper.

In Section 2 we show the main features of the COMPASS-U device relevant to its diagnostics designs. Section 3.1 presents the strategy and plans for the development of diagnostics and reviews the diagnostic set for the first plasmas. Proposed distribution of the systems around the vacuum vessel is shown, indicating the (proposed) full set of diagnostics and other tokamak systems. In detail, Section 3.2 provides the status of the development of individual diagnostic systems, including their essential technical aspects. At the end of the article, future possibilities for the further diagnostic development are outlined (Section 4).

2. COMPASS-U tokamak

The COMPASS-U tokamak (major radius $R = 0.894$ m, minor radius $a = 0.27$ m, plasma elongation up to 1.8 and triangularity less than 0.7, toroidal magnetic field B_t on axis up to 5 T, plasma current I_p up to 2 MA, Greenwald density limit $n_G \sim 8 \times 10^{20}$ m^{-3}, 1–3 s long flat-top at full plasma parameters or about 10 s at low plasma performance), see [1] and [2] for main parameters and technical details, is a new compact European mid-size full-metal device equipped with high performance divertor(s) relevant to ITER from the perspective of plasma shapes and high magnetic field. Furthermore, it allows a hot metallic wall operation (early operational phases at 20 °C → the first step towards elevated temperature in the next operational phases at 300 °C → the maximum operational temperature at 500 °C) and is flexible enough to study advanced concepts of plasma facing components (PFC) and divertors, like use of liquid metals, snowflake configurations as well as plasmas with negative triangularity. COMPASS-U will be equipped with both NBI and ECRH heating systems at the level of several MW, providing enough power for reaching H-mode; it is around 0.6 MW of the heating in the ion channel in the case of the scenario #3210, if evaluated using the scaling in [11].

COMPASS-U is designed as a device with fully metallic plasma facing components, in a double divertor configuration, see Fig. 1, and with no presence of carbon since the start of its operation. The upper open tungsten-coated divertor will represent a temporary solution for initial low-performance diverted plasmas, while the closed, bulk tungsten lower divertor will serve for full performance plasmas later on, when heat flux (perpendicular to divertor targets) densities $q_\perp$ can reach 20 MW/m^2 or up to 90 MW/m^2 in transients at the outer strike-point in attached conditions. Therefore, mitigation strategies like detachment are amongst required conditions for the uncooled plasma facing components to survive such discharges. In COMPASS-U, the divertor tiles at both vertical targets will have a fish-scale design similar to ITER monoblocks with a 0.5 mm toroidal bevel to hide the leading edges. The maximum allowed temperature of the bulk tungsten tiles was set to 2000 °C due to tokamak operational reasons, which can be reached in 3 s (maximum COMPASS-U flattop duration) under a constant heat load of $q_\perp = 20$ MW/m^2. For slow transients such as loss of detachment leading to even higher heat loads, the strategy is to sweep the strike-points. This should give us time to react using our interlock system to terminate the discharge, if the surface temperature, despite the sweeping, exceeds the 2000 °C limit.

A low performance operation of COMPASS-U following the first plasmas, named Phase 1, will be limited mainly by installed PFCs. The required set for Phase 1 includes Inner Wall Limiters (IWLs, protruding less into the plasma) and Inner Guard Limiters (IGLs, protruding more) protecting the central column at the high-field side (HFS), allowing the safe formation of circular plasmas. For protection of in-vessel

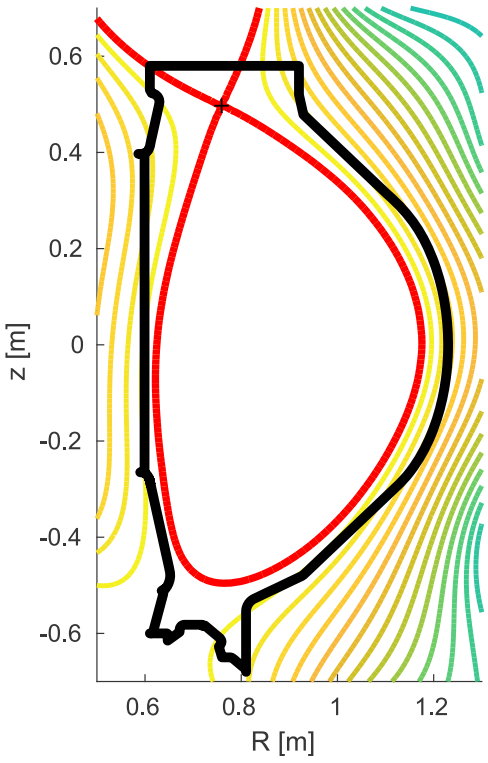

Fig. 1. Magnetic equilibrium for typical operational scenarios of the COMPASS-U tokamak in Phase 1 (#3210 – early H-mode; a very similar one is for #3100 – L-mode). The equilibrium is shown together with the proposed PFCs for later operational phases but only IGLs / IWLs, OGLs / IWLs and the upper divertor will be present there for Phase 1.

components at the opposite side of the vessel, i.e. at low-field side (LFS), toroidally and poloidally discrete crescent-shaped Outer Wall Limiters (OWL, protecting diagnostic ports at midplane) and Outer Guard Limiter (OGL, protecting the vertical connection of the upper and lower Passive Stabilising Plates (PSP) and acting as a barrier for possibly present runaway electrons) will be installed. For testing the first diverted plasmas at low plasma performance, an upper open divertor in the form of a flat toroidal ring is considered for Phase 1, as already mentioned. In Phase 1, the vacuum vessel will be baked up to 150–200 °C for conditioning purposes but kept at room temperature during the discharges. Planned scenarios [12] for this phase are constrained by the installed PFCs and by the absence of the lower divertor, by the available electrical power - 3 flywheels allowing an operation up to 1.25 MA of plasma current and/or 3 T of toroidal magnetic field, and by the initial auxiliary heating systems - 1 MW of NBI power [13], and likely also 1 MW of the ECRH power. Thus, upper single-null diverted configuration in L-mode (scenario #3100) and H-mode (scenario #3210) with $B_t = 2.5$ T and $I_p = 0.8$ MA are considered, see the corresponding magnetic equilibrium simulated by the FIESTA code [14] in Fig. 1 and the density and temperature profiles calculated by METIS [15] in Fig. 2. The calculation of the Phase 1 scenario #3210 was done at 2.6 MW of heating power for a corresponding lower single null configuration with the closed divertor. This certainly gives an upper estimate of the plasma performance, as real performance with an initial open divertor is expected to be lower by 25% at least [16]. The discharge duration will reach up to 3 s in total, probably again constrained mainly by heating of PFCs, including about 0.5 s of the ramp-up and ramp-down phases each.

3. Diagnostics of COMPASS-U

3.1. Strategy of the diagnostic development and first plasma diagnostics

The main constraint for diagnostics is clearly the compatibility with the tokamak operation at elevated temperatures up to 300 °C or 500 °C depending on the stage of operation, that excludes the use of a number of technological solutions commonly used in magnetic confinement fusion. The design of the sensors works with two different approaches to overcome this additional requirement - use of high-temperature compatible materials as exemplified by the in-vessel magnetic diagnostics in Section 3.2.1, or active cooling of non-compatible components as exemplified by the bolometric and soft X-ray detectors in Section 3.2.3. Both of the solutions carry some limitations, however. Although the cooled inserts will be kept as isolated as possible from the surrounding hot vacuum vessel and port extensions by encapsulation of multi-layered thermal shields, the insulation is not perfect and thus the cooled inserts need to be used conservatively. On the other hand, technology of high-temperature compatible cabling for COMPASS-U is notably different from the Kapton-insulated radiation resistant cabling solution proposed for the cooled detectors [17]. While the Kapton insulation can continuously operate under temperatures ranging from cryogenic to about 300 ℃ (and up to 400 ℃ transiently), making it an optimal solution for a majority of fusion devices, its use in COMPASS-U is limited to in-vessel use for the duration of Phase 1 only, for the cooled inserts or near the cryostat edge.

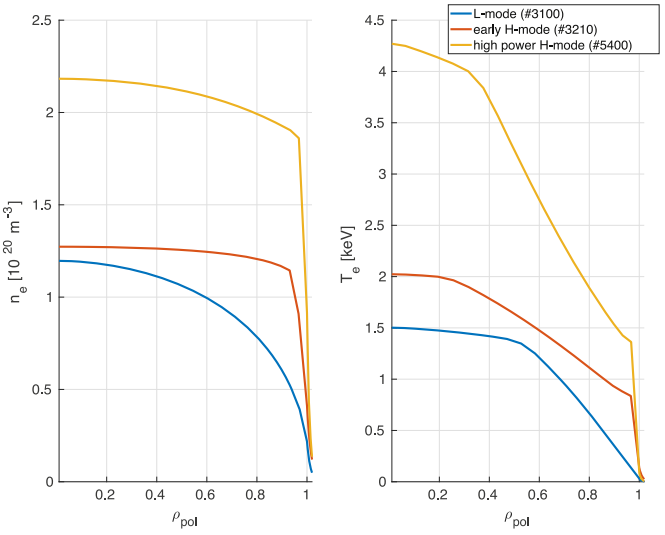

Fig. 2. METIS simulations show density and temperature profiles for the Phase 1 scenarios (#3100 in blue for early L-mode and #3210 in red for early H-mode), including full performance H-mode (scenario #5400 in yellow) that will be realised in later phases for comparison.

A solution for the in-vessel cabling at nominal operational temperatures of the device is presented by fibreglass insulated cables, commonly used in thermocouples. Although some particular fibreglass braids may survive temperatures as high as 800 – 1100 °C, a special care needs to be given when choosing the right product as this high-temperature resistance is, by no means, a universal property of this insulation type (unlike the mineral insulation described later). Use of commonly available fibreglass insulation should not extend above 300 – 400 ℃ as beyond this point we have observed partial melting and sudden drop in the quality of insulation resistance of these materials. Other features of the fibreglass insulated cables to be mindful of relate to their vacuum compatibility, see also [18]. Typically, impregnation compounds are involved in the process of the braiding of the insulation that need to be ideally removed first either chemically or by exposure to elevated temperature in air. Furthermore, the large surface of the braided fibre insulation can slow down the process of evacuation of the vacuum vessel.

A mineral insulated cable (MIC) presents another viable option for in-vessel diagnostic cabling in a temperature range of 300 – 600 ℃ [19]. There, the central conductor is insulated by a compressed ceramic powder, which in turn is encapsulated inside a thin (316 L) stainless steel sheath in a coaxial configuration. As an insulation powder, MgO has been successfully used in other tokamak devices for decades (see references in Section 3.2.1) and is thus also planned for COMPASS-U. However, for higher radiation fluxes such as in ITER compressed alumina powder will be used instead [20]. The most notable drawback when using the MIC cable in a vacuum environment relates to the ceramic powder inside that should not be exposed to the vacuum. Although off-the-shelf MIC terminations are available, it is typically a good practice to avoid termination of the MIC cable inside a tokamak vessel, especially if high temperature thermal cycling above 300 °C is expected during the operation or wall conditioning. MIC port feed-throughs of such devices lead the MIC uninterrupted out of high vacuum into a separately pumped volume, where and only there they are terminated, e.g. DIII-D [8]. This solution is also being considered for COMPASS-U. Alternatively, the MIC might be terminated in vacuum at both ends but only at lower temperatures of about 100 °C (for COMPASS-U in the mouth of the port extensions) and connected to a special (multi-pin) feedthrough [21] or to a Kapton-insulated or fibreglass insulated cable leading to a standard (multi-pin) feedthrough. The MIC termination design will be further reported in a later publication.

A very important point for nearly all tokamak subsystems including diagnostics, widely spread around the vacuum vessel in the tokamak hall but also often reaching neighbouring rooms, is a grounding scheme. The vacuum vessel of COMPASS-U is planned to be electrically connected with the cryostat, forming a common node called Torus Earth. Connection of the Torus Earth to the Building Earth Grid is adjustable - there can be either hard (direct), soft (via resistor) or no connection at all (meaning the Torus Earth is floating). Powerful subsystems, like the auxiliary heating systems, will be locally electrically insulated from the vacuum vessel and grounded separately to the Building Earth Grid. Particular diagnostic grounds for the in-vessel diagnostics will be derived from a local electrical connection with the vacuum vessel near

the position of each diagnostic to ensure no electric arc issues will arise during the tokamak operation (a conductive outer shell of the MIC cables will be naturally connected with the vacuum vessel and its electrical break will be realised within a vacuum feedthrough). In the case of locally electrically floating diagnostics, common grounding points of the corresponding toroidal section will be used to avoid/minimise ground loops as well as arcing issues. Only globally electrically insulated diagnostics are not grounded directly to the Torus Earth; those have their own separate Clean Earth Grid not connected to the main Building Earth Grid to minimise noise propagation from other electrical systems.

A typical constraint for fusion devices with a strong auxiliary heating and a high magnetic field, relevant to ITER and DEMO, are extreme heat fluxes impacting on PFCs. Although for long-pulse machines an active cooling of PFCs is a must, the stationary heat flux still should not exceed 1 – 10 MW/m^2 (depending on its location and a PFC design) or hundreds of MW/m^2 up to tens of GW/m^2 transiently to avoid partial melting and damage of the PFC tiles. COMPASS-U, with its expected steady-state heat flux densities of up to $q_\perp = 20$ MW/m^2 (in a detached divertor regime which is foreseen for nominal operation) for a few seconds long discharge flat-top or up to $q_\perp = 90$ MW/m^2 in a peak for a very short time on the outer divertor target, will allow testing PFC survivability under DEMO-relevant conditions. Thus, diagnostics embedded in PFCs should either survive such extreme conditions or must be shielded against the heat flux by surrounding limiters. Consequently, this will limit a design of diagnostic probes to a flush-mounted concept as discussed in Section 3.2.4. In a divertor with a well stable and small angle of incidence bigger than 0.5°, the flush-mounted rail probes (prolonged to a few cm along the field line) [22] solve issues of the sheath expansion, making measurements in this region credible. The density feedback will be provided by a sub-mm microwave interferometer. In order to minimise issues with deflection of the beam due its refraction as it propagates through plasma, the vertical beam trajectory was abandoned for the sake of horizontal one (as this set-up is less sensitive to the plasma shaping), utilising a reflecting mirror on the HFS in place of two of the PFC tiles. This mirror is possible to be located there due to a (heat) shielding effect of IGLs, protruding more towards the plasma by several millimetres, thus, not allowing an increase of the temperature of the SS mirror above 750 °C.

Another COMPASS-U feature is a high plasma density of the order of 10^{20} m^{-3}. A density measurement at COMPASS-U provided by the interferometer [23] should be reliable for densities up to the Greenwald density limit $n_G \sim 8 \times 10^{20}$ m^{-3}. This can be done with choosing the probing wave frequency above 300 GHz. Taking into account an effect caused by O- and X-mode mixing, injected microwave beams at 498.3/500 GHz provide a safe margin for reliable implementation of the two frequency interferometer with an unambiguous channel, i.e. avoiding fringes, see Fig 3. An expected phase sensitivity is 2.2×10^{18} m^{-3}/1°.

High-temperature plasmas of tokamaks are strong sources of different types of hard radiation, including neutrons, alphas, hard X-ray and gamma radiation. Hard radiation can lead to a parasitic signal in detectors or causes deterioration of properties of the used materials. For optical materials, effects of the radiation induced optical absorption (RIA) and radiation induced luminescence (RIL) have been widely investigated for ITER [24]. It was found that a partial recovery of original optical properties, e.g. of optical fibres, can be reached using either by thermal annealing at temperatures of about 300–500 °C or by photobleaching using UV radiation (but effective only up to 400 nm) [25]. If radiation doses are only moderate like those expected at COMPASS-U (see the next paragraph), use of radiation hardened glasses, as at ITER [26], is the optimum way but a regular exchange of the affected components (in about several years) can represent a cost-effective and also acceptable option.

The auxiliary heating systems of COMPASS-U will be represented by Neutral Beam Injectors (NBI) and Electron Cyclotron Resonance Heating systems (ECRH). More precisely, the design includes three new double

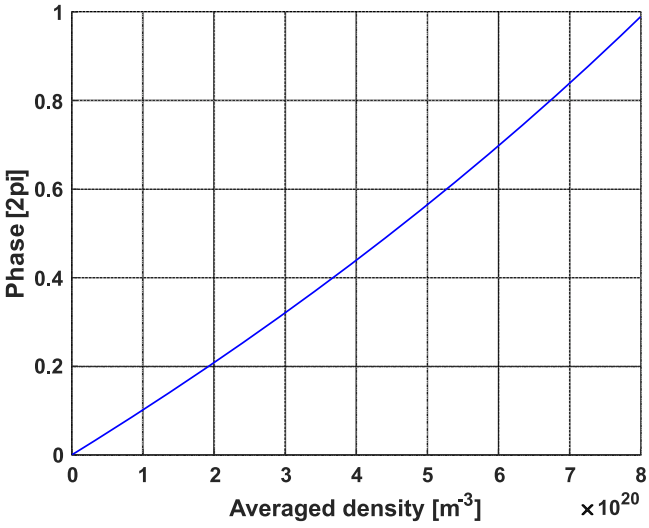

Fig. 3. Expected measured phase of the interferometer working with 500 GHz probing wave as a function of the line-averaged density on COMPASS-U.

NBI units containing six 1 MW (< 80 keV, < 22 A) units in total, plus one such previously used on the COMPASS tokamak [27], as well as two 300 kW beams from COMPASS. Monte Carlo neutron and photon transport (MCNP) simulations of the full performance plasma heated by up to 8 MW of the NBI power indicate that COMPASS-U will become a moderately strong neutron source of up to 2×10^{15} n/s ($\sim 4 \times 10^{19}$ n/year), similar to other mid-size tokamaks. Therefore, 1.5 m thick concrete walls (the current 60 cm thick walls will be reinforced by adding 90 cm of borated concrete) will be built around the tokamak hall, limiting the maximum dose outside to about 6 mSv/y [28]. For this reason, straight openings through the tokamak hall walls for diagnostics with a direct view of the vacuum vessel will be limited to four (for neutron and UV-USX diagnostics only); the rest of the ducts will feature labyrinth-like paths shielded either by the concrete floor in the hall or by dedicated shielding blocks. Whenever it is possible, optical fibres will be used to either a) move sensors and electronics far away from the tokamak to a well shielded area, or b) provide electrical insulation of diagnostics from the tokamak vessel. Both these functions are fulfilled by Fibre Bragg Grating (FBG) diagnostic, providing temperature measurements of the PFCs. At COMPASS-U, high-temperature compatible FBGs will be used and exposed up to 10^{14} n/cm^2/y (while literature [29–31] shows neutron and gamma exposure effects caused by a few orders higher doses, and [32] demonstrates their use in a mid-size tokamak environment).

Stray magnetic field in the tokamak hall presents another design constraint for diagnostics outside of the tokamak vessel or cryostat. A rough estimate with the dipole approximation gives about 10 mT at 6 m distance away from the vessel, at the location of HXR detectors. Thus, about 1 cm thick shielding of these scintillation detectors will be utilised, see Fig 4.

Considering all the above mentioned constraints and real possibilities for a (re)construction of the COMPASS-U diagnostics, we created a set of the first plasma and Phase 1 diagnostics, see Table 1. Including also most probable future diagnostics and systems at COMPASS-U, we prepared a scheme of their distribution, see Fig. 5

3.2. Development of individual diagnostics

3.2.1. Set of magnetic diagnostics

To provide the essential magnetic measurements for the reconstruction of the plasma position and equilibrium from Phase 1 on, COMPASS-U will be equipped with an extensive set of inductive loops and probes. These will measure localised magnetic flux (poloidal Ψ, or

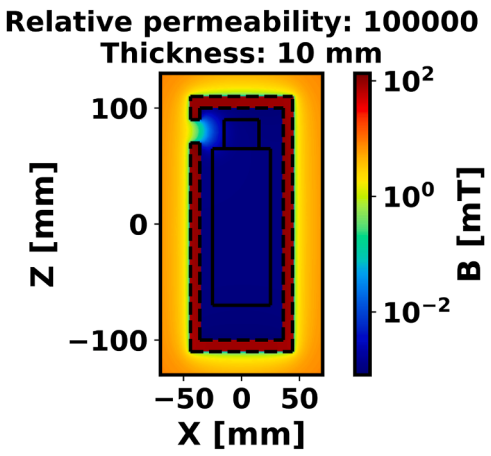

Fig. 4. Example calculation of shielding of the scintillation detector against the 10 mT strong, vertically orientated stray magnetic field from COMPASS-U near the tokamak hall wall. Cross section of the shielding cover with the entrance aperture, located near the top left corner, is displayed by a dashed line. The detector, composed of the scintillator (the top part) and the photomultiplier tube (represented by the bottom rectangle), is marked by a solid line.

Table 1
List of the first plasma and Phase 1 diagnostics planned for the COMPASS-U tokamak. The Phase 1 diagnostics (indicated by stars) will be installed when ready but during Phase 1 at latest.

Magnetic diagnostics - Basic set of magnetic diagnostics: poloidal Flux Loops, 1D and 2D MIC pick-up coils (equilibrium reconstruction, in-vessel Partial Rogowski coil array, B_t detection arrays, toroidal array at LFS midplane), saddle loop toroidal arrays, Thick Printed Copper coils, in-vessel long-segment Rogowski coils (poloidal and toroidal orientation), diamagnetic loops with compensation loops, resistive shunts for halo currents detection, ex-vessel Partial Rogowski coil (poloidal orientation), ex-vessel long segment Rogowski coil
Microwave diagnostics - Microwave interferometer, Reflectometer*, Electron Cyclotron Emission*
Optical diagnostics - Impurity/working gas monitor (VIS/NIR/NUV spectroscopy), Hard X-Ray flux monitors, overview & interlock cameras (VIS/NIR), core & edge Thomson Scattering*, ⟨Zeff⟩ diagnostic*, metallic bolometers*, AXUV diodes ("fast bolometers") *, Soft X-Ray detectors*, IR cameras for IWL thermography*
Particle diagnostics - Neutron flux monitors, Neutral Particle analyzer*
Electric probe diagnostics - Probes embedded in limiters, horiz. recipr. manipulator*, test set of divertor probes*
Diagnostics of Plasma Facing Components - Fibre Bragg Gratings*, surface thermocouples*

toroidal Φ), its spatial derivations ($B_\theta \sim \partial\Psi/\partial\mathbf{x}$), or their line integral quantities ($\int \mathbf{B}_\theta \cdot d\mathbf{l}$) in the vacuum region outside of plasma. The relation of these quantities to magnetic equilibrium and related global plasma parameters is discussed more in detail in [33]. Fig. 6 left shows the distribution of sensors involved in plasma position and shape control, as well as in equilibrium reconstruction. As illustrated in Fig. 6 left, even the first plasma operation sensors feature a high degree of redundancy, in order to ensure uninterrupted operation even in the case of a major fault of an entire sensor array. Two independent poloidal flux loop arrays are installed on the VV from inside, at the same positions next to each other but with signal leads connected to different ports. Two identical, opposite arrays of magnetic pick-up coils with one-axis ("1D coils") and two-axes ("2D coils") sit behind the first wall structures to measure local poloidal component of the magnetic field close to the plasma, and are further complemented by partial Rogowski coil systems installed both in-VV and ex-VV. A set of 2D Thick Printed Copper (TPC - the technology known from power electronics with highest reliability requirements [34]) coils, see their description in the next paragraphs, will also be installed from the first plasma (not shown in the figure), providing further contingency for measurement of the local magnetic fields. The plasma current is to be primarily measured by a continuous Rogowski coil (albeit split into 4 segments in a close contact) and can be contingently measured by a 4 segment Rogowski coil ex-vessel, or by partial Rogowski coil arrays, toroidally opposite to it - both in- and ex-vessel; as well as by the 1D and 2D pick-up coil arrays. Plasma thermal energy is to be measured by three toroidally separate diamagnetic loops, each with their own compensation loop. Two toroidally opposite 1D coil sets installed on the inboard side of the VV (not shown) orientated to measure B_t serve as a contingency for the diamagnet compensation loops.

To evaluate the electromagnetic forces acting on the VV during transient events such as disruptions, measurement of the currents flowing in the VV and their spatial distribution is necessary. Several arrays of 1D MIC magnetic pick-up coils will thus be used to detect local poloidal and toroidal magnetic flux variations across the VV in order to reconstruct the vessel current distribution and, in the later stages, also the currents flowing in the passive stabilising plates (PSP). The total current flowing in the vessel will be extracted from the assembly of in- and ex-vessel long segment Rogowski coils, as shown in Fig. 6 left. The arrays of in- and ex-vessel partial Rogowski coils toroidally opposite to them will be used both to extract the total VV current (and to infer possible $n = 1$ asymmetry) and its spatial distribution in the poloidal direction. A toroidal array of shorter narrow Rogowski coil segments will be installed on the top and bottom of the VV central column to monitor the toroidal distribution of vertical VV currents (not shown) during disruptions. This array will be also supported by the two B_t-detection orientated, toroidally opposite 1D coil arrays mentioned earlier in this section. Direct current flow from the plasma to the vessel will be measured by resistive shunts installed on modified PFC tiles at multiple toroidal and poloidal locations.

Besides diagnosing the basic plasma parameters, the magnetic equilibrium, and the vessel currents, Phase 1 sensors will also have capability to measure plasma magnetic field asymmetries and high frequency oscillations. For detection of slowly rotating and non-rotating plasma MHD structures, COMPASS-U will be equipped with toroidal arrays of saddle loops around the midplane - both on the LFS and the HFS (in later phases of operation, two more arrays will be added behind the PSP). These measurements will be complemented by a toroidal array of 2D MIC pick-up coils installed at the LFS midplane as well as with the equilibrium sensor arrays shown in Fig. 6 left (utilising their $n = 1$ symmetry). At a later commissioning stage, 2D Mirnov coil arrays as shown in Fig. 6 right will be installed around the VV at several toroidal locations to detect high frequency, high-m and high-n structure plasma oscillations. For an early detection of high-frequency plasma instabilities, a TPC coil poloidal array will be operational from the first plasma.

TPC coils are based on technology allowing metallization of ceramic substrates [35]. It allows high flexibility in terms of used ceramic substrates and thickness of copper layer. Resulting metallized structures offer significantly higher heat shock resistance compared to the alternative metallization technologies like Direct Bond Copper, Direct Plated Copper or High/Low Temperature Cofired Ceramics [36]. Moreover, it allows multi stacking of individual metalized substrates with reliable conductive interconnections. As such, TPC technology provides a very attractive concept for development of robust magnetic sensors compatible with operation at high temperature. Commissioning of TPC sensors at COMPASS-U will represent the first of a kind installation of such coils in any fusion device. Main benefits of the COMPASS-U TPC coils (see Fig. 8) for high-frequency plasma instabilities detection include a low capacity (16 pF), a linear frequency response up to 1 MHz and a high effective area (of about 110 cm^2) in combination with a small size (7×15×40 mm). The sensors will be deployed in 2D setup (2 orthogonal coils) and at a certain number of measurement locations the TPC coil will be integrated with Antimony Hall sensors [37] taking advantage of complementary coverage of the measured magnetic field frequency spectrum by these two types of magnetic sensors.

Majority of the magnetic diagnostic sensors will be installed on the

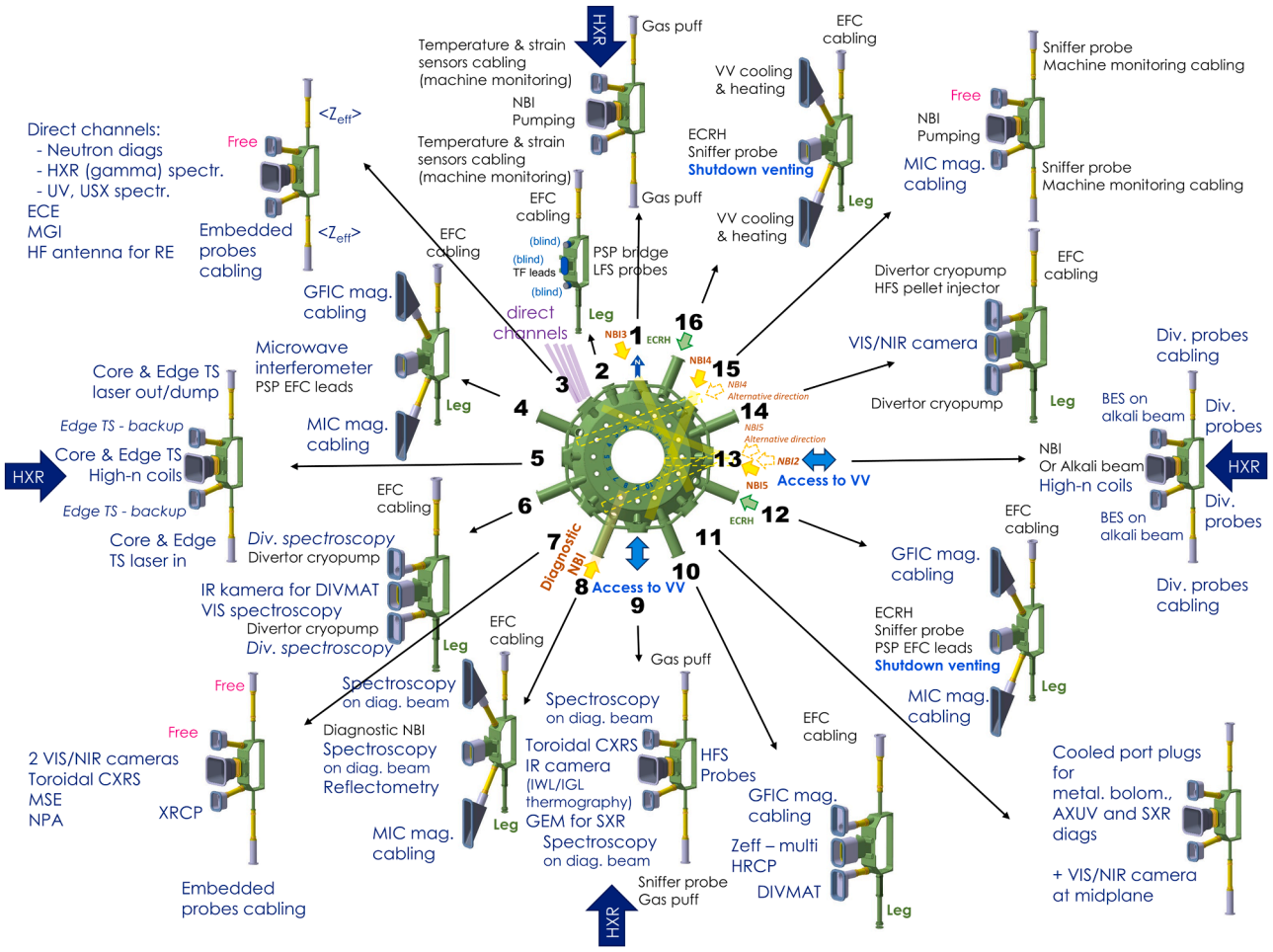

Fig. 5. Scheme of the system distribution around the vacuum vessel of COMPASS-U. The diagnostics to be installed before or during Phase 1 and their expected extensions are indicated by the dark blue colour. Future sets of the diagnostics will be campaign-orientated, thus, the indicated scheme is expected to be modified and/or extended each time accordingly.

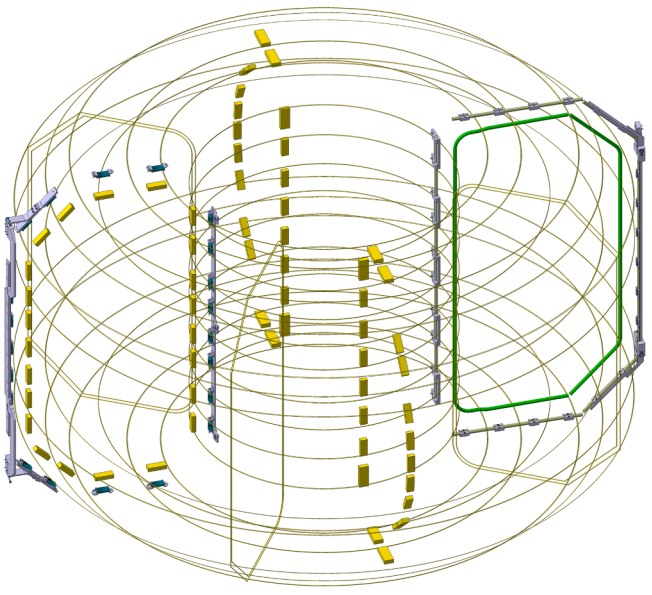

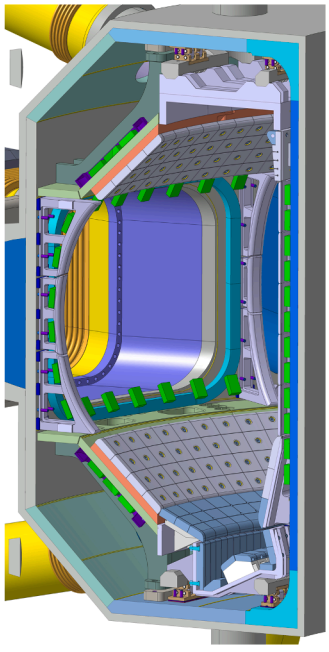

Fig. 6. Left: Distribution of magnetic sensors intended for plasma control and magnetic equilibrium reconstruction operational since the Phase 1 of commissioning. The figure shows positions of poloidal flux loops (toroidal yellow lines), 1D and 2D MIC coils (yellow boxes), diamagnetic loops (poloidal yellow lines), segmented in-vessel Rogowski coil (poloidal green line), and secondary ex-vessel 1D coils and Rogowski segments (grey segments). Right: Integration of magnetic sensors with the VV, PFCs and PSP, demonstrated on a fast 2D Mirnov coil array (green boxes).

inside of the VV, where they will be protected from plasma exposure by PFCs or by their own limiters as illustrated in Fig. 6 right (limiters for toroidal array coils are not shown). The effect of magnetic field signal attenuation by the nearby VV and PFCs has been preliminarily investigated in [38] with the conclusion that the signal from global plasma excursions will not be significantly distorted by the 3D eddy current paths in PFC and can be corrected by a lumped circuit VV model, if necessary. Furthermore, the preliminary modelling in [38] confirms that the inboard-mounted sensors shown in Fig. 6 right will retain their capability to detect plasma oscillations including as far as 50 kHz (which was the maximum frequency investigated in the simulation) thanks to the gaps between the PFC tiles. More detailed analysis on the VV and PFC attenuation will follow in a future work. The available space behind the first wall PFC components also defines the dimensional constraints for the majority of the magnetic sensors, limiting the radius of the Rogowski coils, thickness or width of the 1D and 2D magnetic pick-up coils, etc.

The other defining universal design constraint for magnetic sensors was the 500 ℃ temperature which the sensors and the signal lead cables have to withstand and to successfully operate at. As mentioned in Section 3.1, this leaves two options for the choice of the signal lead cabling insulation - MIC and high-temperature compatible fibreglass. Most of the Phase 1 sensors will be made of continuous MIC making up both the loop and the signal cable lead as shown in Fig. 7, utilising the mechanical robustness of such cable and high reliability as per the experience from other machines such as KSTAR [39], DIII-D [8], TCV [40], etc. The fibreglass-insulated twisted pair cable will be used for signal leads of magnetic sensors whose detection parts are not made of MIC, such as the Rogowski coil segments, fast Mirnov coils (made of uninsulated Cu wire on ceramic mandrel), TPC coils, Hall sensors and the resistive shunts in a similar method as it has been done on e.g. NSTX-U [41]. The ex-vessel sensors, on the other hand, are not subject to the high temperature compatibility requirements, but need to survive and operate at cryogenic temperatures as low as those of liquid nitrogen. For that purpose, the polyimide Kapton insulated cables making up both the detection loops and the signal leads will suffice.

The 1D and 2D pick-up coils intended for equilibrium reconstruction and plasma control will be made of the MIC wound around a 316 L ANSI standard stainless steel support, as shown in Fig. 7. This design decision trades degradation of response to high frequency signals for larger effective area and durability. This results in −3 dB frequency cut-off <20 kHz [42] (more accurate values for the final design will be provided in a later publication), a bandwidth in line with the reported flat frequency response 20 kHz of the KSTAR equilibrium diagnostics system [39]. The survivability of the MIC and of the entire coil assembly up to 500 ℃, as well as the insulation resistance at this temperature have been tested in a heated vacuum chamber. Higher frequency plasma events will be diagnosed by Mirnov coils of bare Cu wire wound on a ceramic mandrel, and by TPC coils. Both have flat frequency response of up to ~1 MHz [42]. Rogowski coil segments will be made of fibreglass-insulated single wire wound around a silica rope. High temperature compatibility tests of the non-MIC sensors and their fibreglass twisted pair lead cables will be conducted in the future.

Most of the magnetic sensors will be precisely calibrated on a dedicated testbench at room temperature before their installation into the tokamak. Furthermore, upon the installation the sensors will be calibrated in-situ on a regular basis under different vessel temperatures (elevated or cryogenic) via discharges of the tokamak coil system. The earlier testbench calibration will then be used as a reference for the in-situ calibration measurements.

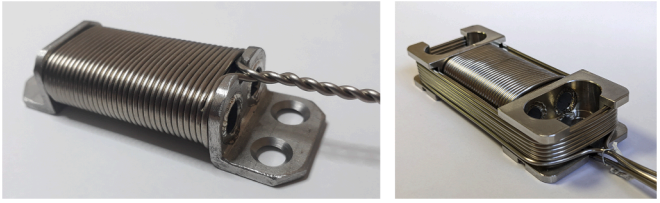

Fig. 7. Prototypes of 1D (left) and 2D (right) MIC coil, respectively.

While the majority of the magnetic sensors will be implemented into the standard COMPASS-U data acquisition with high-frequency sampling rate, the sensors involved in plasma control and equilibrium reconstruction will be real-time numerically integrated and will have their own separate dedicated data acquisition system of a modular architecture. Prototype ADC modules for integration were based on an existing system [43], with incremental developments and up-to-date components. The prototype tests of numerical integration method on the old COMPASS, and the first results of the integrated prototype electronics have been successful and are described in more detail in [44]. The integrator drift was measured at an order of magnitude lower than the 5 μVs/s upper limit (that was obtained from equilibrium reconstruction simulations with COMPASS-U synthetic data).

3.2.2. *Microwave diagnostics including the sub-millimetre interferometer*

Amongst the first plasma and key diagnostics, a one-chord, sub-millimetre interferometer for real-time density feedback will be operated at COMPASS-U, see Fig. 9 and details in [45]. Its concept represents a slightly modified version of the radially directed interferometer equipped with an unambiguous channel proposed in [23], reflecting few newly investigated issues raised from the Conceptual Design Review. The main change is an increase of the probing wave frequencies to 497.3 GHz and 500 GHz, resolving sufficiently the effect of the O- and X-mode fractions mixing during the phase measurement, as described in detail in [45]. The covered line-average densities will range from 1.5×10^{18} to $8 \times 10^{20}\ m^{-3}$.

The proposed design of the interferometer includes the hardware interferometer block (electronics located in the shielded diagnostic room) connected by a quasi-optic line to the semi-flexible oversize waveguide [46] (located in the port insert of the tokamak vacuum vessel). Then, it continues to the corrugated waveguide, minimising transmission losses, and leads to the corrugated receiving and transmitting antennas and the remote-controlled focusing mirror system, being located in the special port insert at atmospheric pressure, see Fig. 9. The high-field-side reflecting mirror is designed as a part of the plasma facing component and placed in the “shadow” of high-field-side guard limiters to reduce plasma interactions.

The waveguide system, based on quasi-optical beam liner, will be used for transferring probing waves from the electronics of the interferometer to the tokamak vacuum vessel and back. The shaped semi-flexible waveguide sections will be used for suppression of the expected vacuum vessel displacements during a discharge as well as those caused by changing operational temperature of the vessel. The remote-controlled focusing mirror system will be based on piezoelectric actuators, allowing a precise system setting in a high magnetic field environment.

For the first plasma and Phase 1 experimental campaigns, a basic set of microwave diagnostics will also be installed to measure kinetic profiles. The microwave reflectometer with a new antenna system inside the vacuum vessel will be employed for the fast density profile measurement. Three O-mode polarised bands: K (18 – 26 GHz), Ka (26 – 40 GHz), and U (40 – 60 GHz) will be arranged in a heterodyne detection scheme [47]. The microwave reflectometer will provide density profile measurements of up to $4 \times 10^{19}\ m^{-3}$ and a temporal resolution of up to 6 μs.

In collaboration with the University of Texas at Austin, an Electron Cyclotron Emission system (ECE) is under development [48] and will allow fast measurements of radial electron temperature profile. The ECE system for Phase 1 is tailored for toroidal magnetic field $B_t = 2.5$ T. A radiometer with 40 channels, frequencies of 110 – 160 GHz and 500 MHz channel bandwidth covers the plasma radius of $-0.38 < r/a < 1.1$. The quasioptical (QO) antenna system with two elliptical mirrors and a

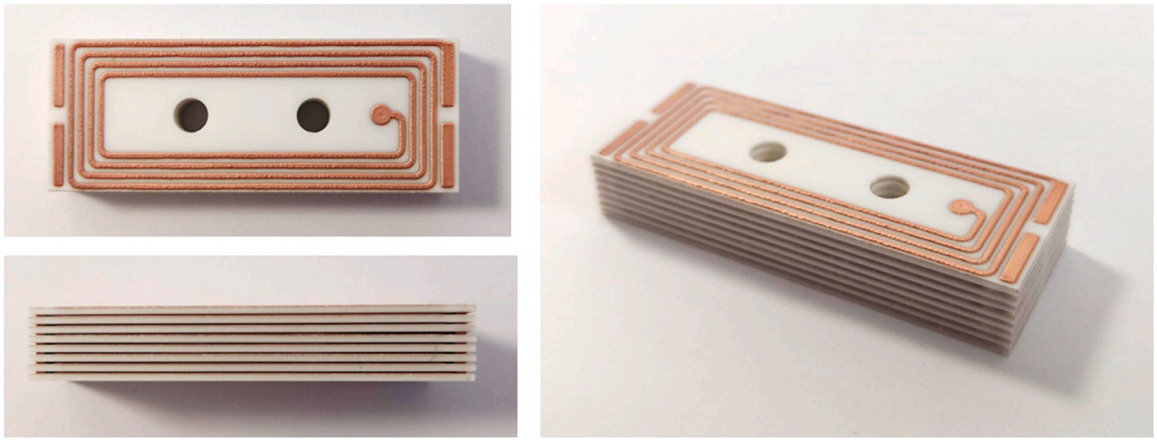

Fig. 8. Prototypes of TPC coils.

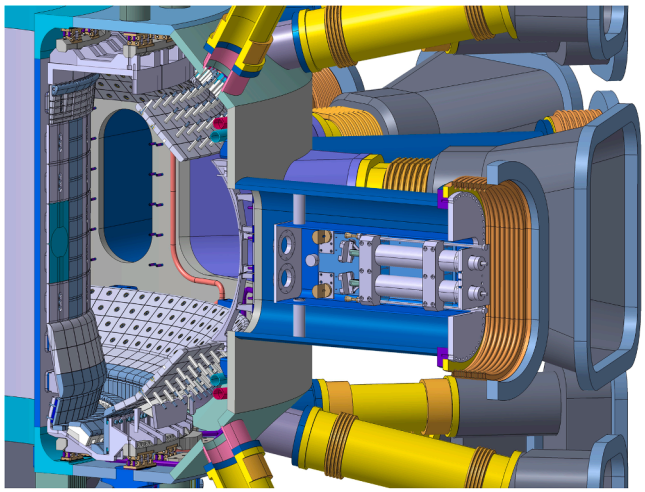

Fig. 9. Poloidal cut of the vacuum vessel section dedicated to the sub-millimetre interferometer. On the left, the high field side reflecting mirror (green) is aligned with neighbouring plasma facing components. On the right, the port insert (blue) contains the antenna front-end with a remote-controlled focusing system (grey parts).

hot calibration source will be placed outside the cryostat. The vacuum window followed by the aperture made from SiC will define the incoming Gaussian beam. For the next phase with $B_t = 5$ T, a new radiometer with frequencies 215 – 306 GHz is needed. The QO antenna system, hot calibration source, and waveguides stay the same.

All microwave diagnostics will be protected from the stray microwave radiation from the future ECRH system.

3.2.3. *Optical and radiation diagnostics*

In order to overview plasma discharges and monitor the first wall of COMPASS-U, four sets of visible light and near-infrared (NIR, ~1 μm) cameras will be installed around the tokamak, trying to achieve the maximum coverage of all plasma facing components (PFCs), see Fig. 10. They will observe plasma-surface interaction and, in particular, all low field side limiters, both up and down divertors and neutral beam injection paths and beam dumps at frame rates between 100 and 1000 frames per second. For Phase 1, real-time camera operation is not foreseen, as plasma parameters should be low enough to avoid major PFC damages, while a real-time hot spot detection system should be implemented for high performance phases. It is expected that the cameras will not be much influenced by the neutron flux in Phase 1, however, pixels saturated as a result of such an interaction with neutrons or

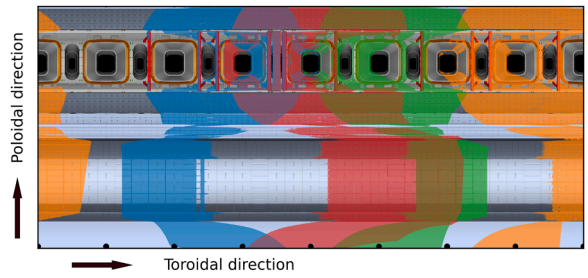

Fig. 10. Coverage of PFCs by near-infrared and visible light cameras; each camera view is represented by a different colour (red, orange, green, blue). Toroidal coordinate is in the horizontal direction, the poloidal coordinate in the vertical direction. The top half of the figure shows the LFS equipped with big diagnostic ports at the midplane, the bottom half visualizes the HFS PFCs.

gammas will be excluded from the real-time data processing by a filtering algorithm.

For the four camera sets, the optical designs are based on the same concept: the first mirror, resistant to high temperatures (up to 500 °C), will collect the light from the plasma, which will be then guided by other mirrors through the port. The use of a Cassegrain telescope is foreseen to allow for a larger field-of-view. Since the design relies only on mirrors, components for the visible and NIR radiation will share the same optical path, keeping the design as compact as possible. A beam splitter will then separate these two spectral components and guide them towards two separated collecting sensors (silicon chips, sensitive to both visible and near infrared radiation).

Based on previous designs, three concepts of the first mirror are being envisaged: a set of two parabolic mirrors [49], a set of two spherical mirrors [50] or the use of a hyperbolic mirror [51]. The retained design will be a compromise between the occupied port space (small ports and other diagnostics sharing them) and the achievable field-of-view (~70 degrees in the vertical direction) and spatial resolution (~ 4 mm). At the time of writing, the visible light and near-infrared camera diagnostic design is still under development.

A fast medium wavelength infrared camera (3 – 5.5 μm) [52] will be used for monitoring tungsten inner guard limiters located at the central column of the COMPASS-U vacuum vessel. The camera will be located at one of the outer midplane MX ports with a direct view to the limiters through a sapphire vacuum viewport. The camera will provide up to 2000 frames per second with 320 × 256 pixel resolution.

The radiated power on COMPASS-U will be measured in one poloidal cross-section by two systems: metallic bolometers and AXUV diodes acting as fast bolometers [53]. Metallic bolometers will be based on four-channel resistive foil bolometers with Au absorber, silicon nitride

substrate and Pt resistor. They allow for absolutely calibrated spatially and time-resolved measurement due to the possibility of self-calibration. Metallic bolometers aim at monitoring slow phenomena like detachment (~ 5 ms). The primary purpose of AXUV diodes is to observe fast events like ELMs or MHD activities. Additionally, fast bolometers cameras will be used for toroidal asymmetries studies. The application of pinhole cameras reduces the number of openings in the PFCs. The cameras will consist of two kinds of detectors located side by side that allows for cross-calibration between the diagnostics. In the initial part of the system, two cameras will be placed in the midplane port plug to observe the plasma core. In the later phases of the tokamak operation, the cameras above the upper divertor and near the lower divertor will be positioned. The full metallic bolometers diagnostics will consist of 32 channels. The core part will have a 2.5 cm resolution. The AXUV diodes system will be composed of 120 channels with a spatial resolution of about 1 cm. All cameras will require temperature monitoring and an efficient active cooling system. In front of the cameras will be placed radiation shielding made by Inconel, possibly silvered to increase the reflectivity. The whole midplane port plug will be cooled by air, and small inserts with the cameras will be equipped with additional cooling pipes. The safe operation temperature for metallic bolometers is 200 °C. The temperature around AXUV diodes needs to be lower than 80 °C. Similar conditions are required by PCB amplifiers which will be placed as close as possible to the diodes inside the port. Both diagnostics will be connected with DAQs by Kapton cables that can sustain at least 250 °C. If the cooling systems are insufficient, the detectors from problematic areas will be removed.

For measurements of soft X-ray radiation AXUV photodiode arrays equipped with a beryllium filter are proposed [17]. It is planned to have two sets of arrays with the same coverage of plasma. Each set is equipped with a different filter enabling use of the Ratio method for electron temperature estimation. This system will share an engineering design with AXUV bolometers and the same strategy for the first plasma operation. The full system should consist of 100 channels for each filter, making in total 200 channels.

Measurement of the hard X-ray flux during first phases of COMPASS-U operation will be realised by a set of four scintillation detectors placed inside the experimental hall, distributed by 90° toroidally. The scintillation detector consists of a scintillation crystal coupled to a photomultiplier tube. As a scintillation material $CeBr_3$ was chosen due to its short decay time (20 ns) and good energy resolution. This diagnostic should play an important role in runaway electron experiments but also would be useful for scenario development in Phase 1. Due to the presence of stray magnetic fields (up to 10 mT), the photomultiplier tube will be additionally shielded to suppress change in gain and secure reliable operation of detectors. Also, one HXR spectrometer with a dedicated direct line of sight is planned and will be optimised for runaway electron studies.

Thomson scattering (TS) diagnostic for measurement of electron temperature and density profiles in the core and edge plasma is being designed [54,55] and is expected to be implemented during Phase 1, at least the part of the system observing the core plasma. The TS system will re-use four Nd:YAG lasers (1.5 J pulse energy and 30 Hz repetition rate each), 29 polychromators and 120 channels of the 1 GS/s data acquisition from the COMPASS TS system. New lenses, separate for core and edge plasmas, will be built. New fibre bundles will be procured, not only to optimise the bundle shape and size, but also to reach new diagnostic rooms, located further from the tokamak, through the routes compatible with increased radiation shielding requirements. The requirement on the TS system field of view was recently revised; due to the limited space in the tokamak midplane port it is preferred to cover only a half of the plasma cross-section (i.e. from centre to the edge) with a higher optical throughput, over the full plasma diameter coverage that would lead to a compromised system performance. The collection lenses will utilise radiation hardened glasses. The collection optics will not be exposed to high thermal loads during Phase 1, but the design is considering later phases and methods to lower the thermal loads and to extend the operational temperatures of the used optics. The number of available polychromators and data acquisition channels will limit the coverage of the edge plasma region in the initial operational phase, thus, a region of interest will have to be selected prior to the experiment and fibre bundles at corresponding positions will be connected. An increase of TS measurement points, i.e. number of fibre bundles, polychromators and data acquisition channels, will be required in the later phases, to fully cover the edge plasma region.

Overall information on plasma impurities will be delivered by the effective ion charge (Z_{eff}) diagnostic. It will be realised using the measurement of the Bremsstrahlung continuum in the visible light line-free region. A relatively simple but robust system consisting of collection optics and optical fibres coupled to a photomultiplier tube is foreseen and being designed. For Phase 1 of the tokamak operation, only one vertical line of sight is expected, thus, line average effective ion charge $\langle Z_{eff} \rangle$ will be evaluated. Possibilities for the multi-channel (Z_{eff} profile) diagnostic will be considered in the next operational phases.

A detailed investigation of plasma impurities will be done using several optical channels for spectroscopy in visible light, near ultraviolet and near infrared regions. This will provide information about plasma composition, MHD activity, impurities inflow and recycling processes since the first plasma. Collecting optics made from fused silica (e.g. Suprasil is also a radiation resistant material) will be protected by a high temperature-resilient sapphire window (C axis, Ky or HEM). Detectors, being sensitive to elevated temperatures, magnetic field as well as hard radiation, will be located in a shielded diagnostic room outside the tokamak hall and connected to the collecting optics by 30 – 35 m long high temperature fused silica (Suprasil) core and cladding metal covered optical fibres. The detecting part of the diagnostic system will be represented by a set of high resolution mini spectrometers from Ocean Optics, types HR2000+ and MAYA, allowing measurements in the spectral range of 247 - 1084 nm, and by photomultipliers equipped with interference filters corresponding to individual impurity and hydrogen lines. Presence of metallic walls in COMPASS-U brings a serious issue for optical diagnostics that is currently investigated by our modelling activities - reflections. Thus, a special surface treatment of the observed PFCs is under consideration with the aim to decrease their reflectivity, see e.g. the effect of surface roughness on reflectivity in [56], or, if unavoidable, optical dumps [57] that can mitigate stray light by up to few orders of magnitude will be utilised.

3.2.4. *Electric probe diagnostics*

One of the most commonly used diagnostics in tokamaks to measure local parameters of the edge plasma are Langmuir probes. The Conceptual Design Review of the Langmuir probe diagnostic for the COMPASS-U tokamak first wall (inner and outer limiters, divertor baffles) was passed in spring 2021. Because of the expected high heat fluxes, the diagnostic is based on flush-mounted probes embedded in the limiter tiles. Calculations of the foreseen heat fluxes and angles of incidence at the probes' locations for typical COMPASS-U scenarios

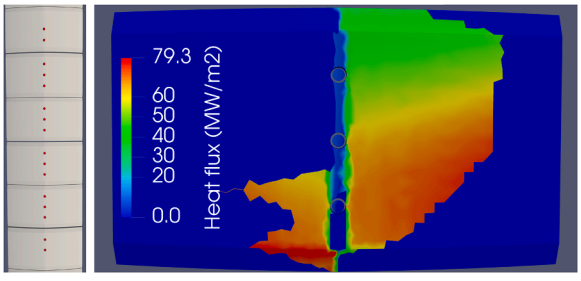

Fig. 11. Probes (red dots) embedded in the IGL (left) and the PFCflux calculations of foreseen heat fluxes near the probes embedded in the tile located just above the tokamak mid-plane (right).

were performed using a 3D field line tracing code, called PFCflux [58], at all poloidal probes positions for optimization, see Fig. 11. Consequently, the flush-mounted probes will have a diameter of 3 mm. Fig. 12 illustrates the proposal including 16 probes (red dots) on the IGL (on the inner 6 tiles, symmetrical 3 tiles up and down from the midplane), with a spatial resolution of 1 – 2 cm, 3 probes on the upper inner divertor baffles at the same toroidal position and 4 on the lower one. Toroidally, they will be placed on the guard limiter in front of the midplane port 9, where the fast infrared camera will observe the HFS plasma. Therefore, probe measurements (heat flux) can be compared with those of the IR camera.

At the LFS, 11 probes (spatial resolution of 5 cm) are planned to be mounted on the OGL next to the bridge protecting the vertical connection of the upper and lower passive stabilising plates, and 4 probes on the lower outer divertor baffle at the same toroidal position (Fig. 12, blue dots). The toroidal position is in the vicinity of the toroidal section 3.

High-temperature MIC cables to connect the probes will be used, since we do not plan for their frequent replacement, while the operating temperature of the vacuum vessel may reach 500 °C.

Another type of flush-mounted probes, which will be embedded directly to the divertor targets, are so-called rail probes [22], being based on the design from Alcator C-Mod [59]. This novel type of probes, resolving issues of the sheath expansion, is capable of withstanding very high parallel heat flux up to 1 GW/m^2.

Indeed, 2D PIC simulations of the particle heat flux incoming to the rail probe surface were performed with the aim to map their behaviour under different conditions (plasma density, electron temperature, magnetic field and its field line inclination). The probe itself is biased by a negative voltage of $-10k_BT_e/e$ to operate in the ion saturation current mode. We also assume the ion and electron temperatures to be equal. In the next step, the resulting distribution of the heat flux on the probe surface is an input for the thermal analysis conducted in COMSOL Multiphysics. A full 3D simulation of heat conduction in a small volume around the probe with radiation exchange was assumed. We have used an expected dimension of the rail probe design for COMPASS-U (length 50 mm in the toroidal direction, width 2 mm, depth 10 mm) enclosed in a tungsten box representing the surrounding tiles. The boundary condition of the simulation was a heat bath at 500 °C. The cooling of the probe by its mechanical attachment was neglected and the results thus represent an upper temperature estimate. Fig. 13 shows an example of the thermal analysis of the maximum probe surface temperature. Here we plot the maximum temperature reached for two different electron temperatures with respect to the plasma density during 5 s. The magnetic field line inclination was set to 1 degree for 5 T, which represents the value expected for the first plasma scenarios on COMPASS-U in the vicinity of the strike point. Note, low temperature values on the strike point are expected only for high density scenarios. We see in the figure that for both cases the maximum probe surface temperature is still below the melting point of tungsten. However, for temperatures above 2 000 °C (the maximum allowed for the divertor tiles) the interlock system will be used. As the last step in the rail probe design, thermomechanically induced stresses will be investigated using an ANSYS analysis to check effects of the fast dynamics of the heating process.

Fig. 14 shows pneumatic reciprocating manipulators designed for COMPASS-U, however, at least in Phase 1, only the horizontal midplane manipulator (HRCP) is considered, while the lower X-point manipulator (XRCP) would only later support the research after installing the lower closed divertor. Both HRCP and XRCP will be equipped with a heat resistant head (∅ < 3 cm shown in Fig 2 in [60]) with a set of Langmuir and ball-pen (BPP) probes, which will allow for fast (1 MHz) and local measurements (1 mm) outside LCFS (assuming plasma density ~10^{20} m^{-3}) [61]. Since at midplane only the probe head tip is exposed to plasma with the predicted exponential 1.3 mm decay length, both the head and rail probes are exposed by a very shallow angle to the plasma. Even ion temperature can be obtained via sweeping BPP every 10^{-5} s

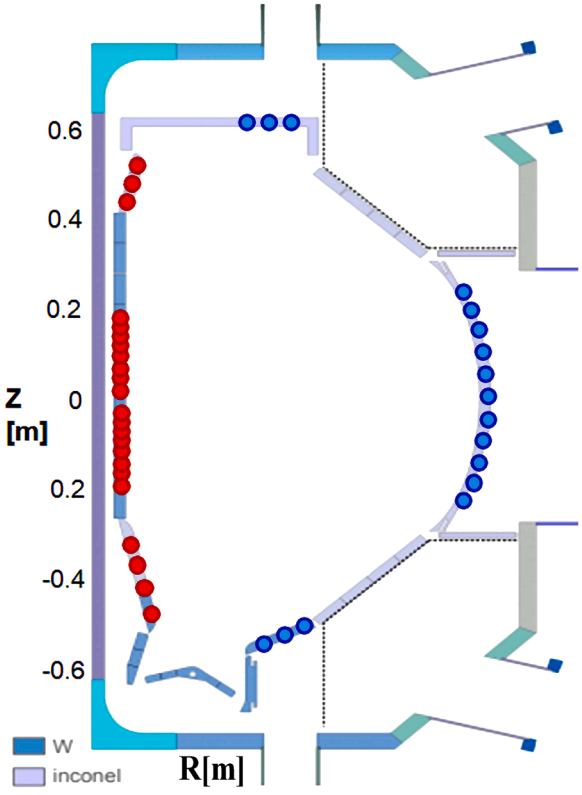

Fig. 12. Proposed poloidal distribution of the embedded flush-mounted probes at COMPASS-U. The red circles represent the probes at HFS in front of the fast infrared camera; the blue circles indicate the probes located at another toroidal position on the vertical connection of the passive stabilising plates.

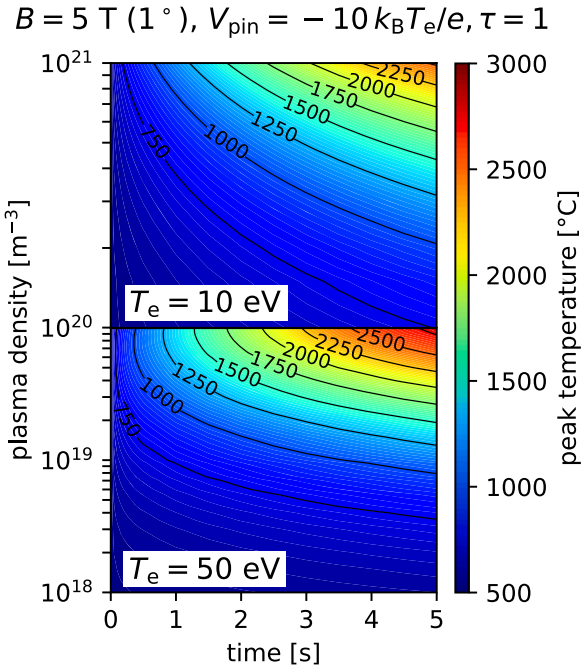

Fig. 13. Example of the thermal analysis of the rail probe surface temperature. The maximum temperature is plotted with respect to the plasma density and the discharge duration for two different electron temperatures and stays well below the melting temperature of tungsten (chosen material of the probe tips) of 3 400 °C. The probe is biased at -10 k_BT_e/e with respect to the plasma potential. The magnetic field is 5 T with inclination 1 degree to the probe surface.

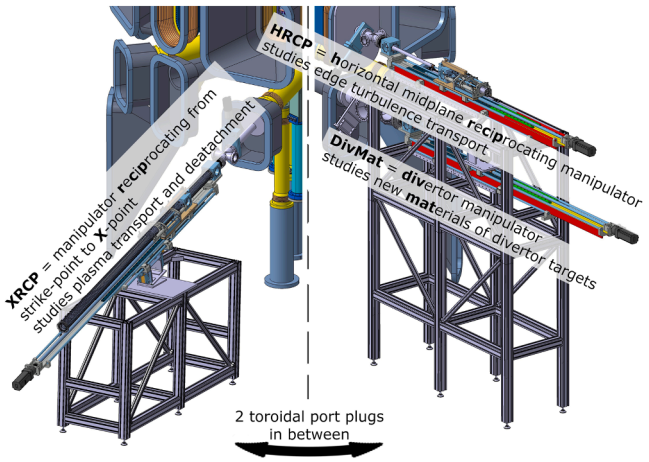

Fig. 14. Detailed design of two fast reciprocating + measuring and one slow manipulator.

[62] revealing statistical properties consistent with theoretical expectations and similar to that of density and electron temperature. Such measurements (plunges) can be repeated 10 times within a 2 s long discharge. Achieving such parameters requires several improvements over the design of previous manipulators on the COMPASS tokamak. In particular, safe real-time motion control uses directly the signal from the probes and the addition of a spring system ensuring maximum possible deceleration a of the probe at the deepest plunge [61]. Unfortunately, the most critical parameter, the probe surface temperature, drops only as $a^{-½}$, thus increase from standard 4g up to too risky 70g ($g = 10$ m/s^2 is the gravity acceleration) decreases the probe (pin) surface temperature only by factor of 2. HRCP arrangement ensures an easy check of any possible head damage through a vacuum window with the possibility of total disconnection of the manipulator and replacement of the head without terminating the tokamak vacuum.

Not reciprocating, otherwise similar manipulator DivMat will be generally used for delivering various test target materials at the outer divertor strike point. Particular care is put on the option to vary the plasma- target incidence angle from 0 to $\pi/2$ on shot-to-shot basis and allow for the target temperature control, both crucial and simulated [63] for a test planned liquid metal target. Even for a medium performance plasma we thus expect to be able to demonstrate survival of a liquid metal target under EU DEMO-relevant plasma steady-state heat flux (160 MW/m^2) and ITER-relevant 20 MJ.m^{-2}.$s^{-1/2}$ ELMs, all perpendicular to the divertor target surface.

3.2.5. Particle diagnostics

The primary system for time-resolved monitoring of neutron emission from COMPASS-U [64] plasma will be based on a set of neutron counters. These neutron flux monitors are designed in collaboration with IFJ PAN, Krakow. This institute also runs the full scale MCNP simulations that are essential for the neutron diagnostics and other radiation-related tasks. The current design aims for 4 neutron flux monitors of optimal sensitivity range that will be accompanied by a neutron activation system and a compact neutron spectrometer, first based on well-proven scintillator design and then replaced by a novel high-resolution instrument using the GEM (gas electron multiplier) principle with a suitable conversion layer. For the flux monitors, a couple of options are still under consideration, including ^{3}He detectors (e.g. Centronic 25He3/380/25) enclosed in a properly designed layer of moderation material, allowing fast neutron detection or suitable solid state detectors with e.g. ^{6}LiF enriched scintillator. These detectors were successfully used in the last campaigns of the COMPASS tokamak and sensitivity optimization with the scintillator volume was achieved, modelled with openMC and proven to be working well in the experiments with 1 MW NBI. Evaluation of the sensitivity and n/gamma discrimination properties of various considered detectors is planned to be conducted using the fast neutron generator (IGN-14) [65] located at IFJ PAN in Poland. The final detailed MCNP simulation with major components and realistic shielding wall composition will also be run in the near future.

In addition, time-integrated monitoring of the neutron flux will be performed by the activation method. The diagnostic is foreseen to be designed and developed for later phases of COMPASS-U operation. The use of neutron activation method for determining the neutron fluence at a given point has a long tradition in tokamak devices. Typically, disk-shaped samples of Ni, Zn, In, Al, Si, Fe or Co are used for activation. However, in the activation system for COMPASS-U, we propose to use Yttrium (Y) samples. This choice is justified mostly by two factors. Firstly, the gamma-ray spectrum features a well-defined line of energy $E_\gamma = 908.96$ keV (intensity of the gamma emission $I_\gamma = 99.16\%$) originating from ^{89}Y(n,n')^{89m}Y reaction with a relatively high cross-section of ~ 1.4 b for 2.5 MeV neutrons and threshold energy of 919 keV. Secondly, the half-life $T_{1/2}$ of the isomeric state is ~ 15.7 s that suits well the expected plasma discharge duration of a few seconds. It is foreseen to use a gamma-ray spectrometer based on $LaBr_3$(Ce) scintillator for the activity measurements of Y samples. The diagnostic design will be strongly supported by Monte Carlo calculation of neutron transport. The primary aspect to be addressed and clarified by calculation results is whether the gamma-ray spectrometer can be located directly in the tokamak hall, with a properly designed shielding from neutron and gamma radiation to avoid radiation damage, or it will be necessary to place the spectrometer further away in the low background radiation environment and apply a sample transportation system.

There are two neutral particle analyzers (NPA) owned by IPP Prague and they will be re-used on the COMPASS-U. Both of them were originally constructed by Ioffe institute [66]. One of them is equipped with 24 detector channels and it is capable of distinguishing hydrogen isotopes. It has 12 channels for hydrogen measuring in the energy range 0.27 - 70 keV and a second row of 12 detectors for deuterium measuring in the energy range 0.3 - 50 keV [67]. The second NPA has 5 channels only and it does not distinguish hydrogen isotopes. On the other hand, it is possible to sweep a sorting electric field, so there can be 5-times more measured points in the resulting energy spectra. The 5-channel NPA measures at the thermal range of the energy spectra only, 0.1 - 7 keV. The 24-channel NPA will be primarily used for the fast ion studies or for the hydrogen isotopes ratio. It is going to be located in the midplane port, segment no. 7 and its line of sight (LOS) will be crossing the diagnostic beam (DNBI). It will allow the measurement of passive signal, coming mostly from the edge region, and active signal, originating from the NPA LOS intersection with DNBI. The 5-channel NPA is not assigned yet to the specific port. It can be used for the ion temperature measurements or for the background neutral density determination [68]. If it is located at or close to the midplane with radial LOS, the measured neutral flux will originate from the region with the normalised radius greater than about 0.8, thus it will provide information about the pedestal region. Regarding the COMPASS-U environment, the detectors should survive the expected neutron fluxes. The upper limit for the NPA detectors is 1×10^{10} n/s/cm^2, which is below the expected value in the NPAs' location 5×10^9 n/s/cm^2. This estimate is a flux value at the NPA port edge based on MCNP6 neutron transport simulations, assuming a neutron yield of the expected high performance scenario and using the main tokamak and shielding structure geometry. To prevent measured neutral flux attenuation inside the connecting pipeline with the tokamak vacuum chamber, the line-integrated gas density inside the pipeline should not exceed 3×10^{19} m^{-2}, which is feasible with the considered NPAs' pumping system.

3.2.6. Diagnostics of plasma facing components

For the measurements of PFC bulk temperature, the Fibre Bragg Grating (FBG) temperature sensors are planned from the first phase of

operation. The FBG sensors use reflection of laser light on gratings inscribed in an optical fibre for temperature and strain sensing. The conceptual design of the FBG sensors is described in the article [69]. The FBG sensors will be embedded in the initial open divertor and both outer and inner guard limiter for good coverage of the plasma heat loads. The fibres are compatible with moderate neutron fluxes expected during the COMPASS-U operation and the high temperature operation of the first wall (500 °C) thanks to their maximum operating temperature of 1200 °C, which was tested at WEST tokamak [70]. The bulk temperature measurements of the closed tungsten divertor by FBG sensors will be complemented by self-renewing surface thermocouple sensors for direct heat flux measurements.

4. Future plans

After securing a basic functionality of the COMPASS-U tokamak and its set of the essential diagnostics, i.e. when Phase 1 is successfully passed, the development of diagnostics will be refocused on an extension of the installed Phase 1 diagnostics (such as Thomson Scattering, magnetics, bolometry & soft X-ray diagnostic, ECE, FBGs, divertor probes and reflectometry) with the aim to improve their spatial resolution by increasing the number of channels and their temporal resolution by technical improvements. In parallel, the diagnostic set will be fully orientated on the physics research. Thus, we will start construction of advanced diagnostics aimed at physics relevant to high heat flux mitigation (detachment), different divertor concepts (liquid metals) and to confinement studies (I-mode), e.g. using high repetition Thomson Scattering, divertor Thomson Scattering, IR cameras for divertor studies, divertor spectroscopy, (H/D or alkali) beam diagnostics like Beam Emission Spectroscopy (BES) & Charge eXchange Recombination Spectroscopy (CXRS) [71] & Motional Stark Effect (MSE), Fast Ion Loss Detector (FILD), X-point & divertor manipulators and Gas Electron Multipliers (GEM).

Upon Phase 1 of commissioning, the magnetic sensor system will be further enhanced to expand beyond simple plasma control studies. Without any need to upgrade the hardware, the original fast Phase 1 plasma shape and position control will be taken over by a real-time equilibrium reconstruction. Two more, toroidally opposed large-segment Rogowski coils will be further installed to enable better plasma current asymmetry measurement. Likewise, the number of diamagnetic loops will be enhanced to 5, having in mind simultaneous plasma diamagnetism measurements close to and away from the NBI position. Upon the installation of the PSP, saddle loops and 1D pick-up coil will be installed behind them, and small Rogowski coils will measure the total current in both of the plates at 4 separate positions. The most notable upgrade would be the installation of the fast 2D Mirnov pick-up coils on the positions as shown in Fig. 6 right. In order to test DEMO-relevant steady-state magnetic field sensors, the developed ceramic-metal Hall sensors [72,73] will be included within the magnetic diagnostics system. The Hall sensors will contribute to the measurement of the plasma current, plasma-wall clearance, and low-frequency < 10 Hz MHD modes. One of the main aims of the installation of the Hall sensors will be to verify the long term performance of the sensors in the tokamak at operating temperatures up to 500 °C [9,15].

In the future we also would like to exploit unique capabilities of a relatively new GEM technology for SXR imaging diagnostics [74] that is expected to have a good spatial resolution of about 100 μm, a time resolution of about 1 ms, a wide dynamic range and an energy discrimination of order of 20–30% in a single photon counting mode. The technology is being developed for a while and is orientated at future fusion reactor applications due to its robustness against radiation damage compared to conventional silicon detectors. As a toroidal camera it can access anisotropic radiation triggered by magnetic reconnection or massive gas injections and serve as a 3D tool for runaway electron studies as well as for plasma shape control.

In addition, the cutting-edge neutron spectrometer, based on a novel concept of GEM-based detector for neutron spectrometry, developed in the framework of the EUROfusion Enabling Research project no. CfP-FSD-AWP21-ENR-04-IPPLM-01, is foreseen to be tested and used in the further phases of COMPASS-U. This high-resolution neutron spectrometer will be able to measure neutron emission spectrum along one (close to tangential) line of sight.

The diagnostics systems will be integrated into and controlled by the COMPASS-U Slow control and supervision system [75]. Therefore, diagnostics will profit from services provided by the Slow control and supervision system such as a unified interface, configuration management (integration into the configuration database), and access management. One of the integration goals is to ease the calibration procedures and diagnostics tests. The way towards this is similar configuration and data handling as from regular experimental discharge, support of mobile devices (user interface run in a web browser), and a possibility to use cross-systems actions and script them.

Declaration of Competing Interest

None.

Data availability

No data was used for the research described in the article.

Acknowledgments

This work has been carried out within the framework of the project COMPASS-U: Tokamak for cutting-edge fusion research (No. CZ.02.1.01/0.0/0.0/16_019/0000768) and co-funded from European structural and investment funds. The authors of the article would also like to thank Robert Ellis and his colleagues from Princeton Plasma Physics Laboratory, USA for fruitful discussions about magnetic diagnostic designs.

References

[1] R. Panek, et al., Fusion Eng. Des. 123 (2017) 11, https://doi.org/10.1016/j.fusengdes.2017.03.002.
[2] P. Vondracek, et al., Fusion Eng. Des. 169 (2021), 112490, https://doi.org/10.1016/j.fusengdes.2021.112490.
[3] V. Weinzettl, et al., Fusion Eng. Des. 146 (2019) 1703, https://doi.org/10.1016/j.fusengdes.2019.03.020.
[4] O. Neubauer, et al., Fusion Sci. Technol. 47 (2005) 76, https://doi.org/10.13182/FST05-A689.
[5] A. Cosler, R. Kurz, G. Waidmann, "Design, fabrication and testing of magnetic field diagnostic components for implantation into the TEXTOR tokamak", Symposium on Engineering Problems of Fusion Research, 8th, San Francisco, Calif., November 13-16, 1979, Proceedings. Volume 4. (A81-18901 06-75) Piscataway, N.J., Institute of Electrical and Electronics Engineers, Inc., 1979, p. 1903-1907.
[6] Mayer, M., Philipps, V., Esser, H.G., Wienhold, P., Rubel, M. (2000). "Wall Pumping and Hydrogen Recycling in TEXTOR 94". In: Wu, C.H. (eds) "Hydrogen Recycling at Plasma Facing Materials". NATO Science Series, vol 1. Springer, Dordrecht. https://doi.org/10.1007/978-94-011-4331-8_2.
[7] P.M. Anderson, A.G. Kellman, Optimized baking of the DIII-D vessel, in: 18th IEEE/NPSS Symposium on Fusion Engineering. Symposium Proceedings (Cat. No.99CH37050, 1999, pp. 535–538, https://doi.org/10.1109/FUSION.1999.849896.
[8] E.J. Strait, Rev. Sci. Instrum. 77 (2006), 023502, https://doi.org/10.1063/1.2166493.
[9] J.G. Bak, S.G. Lee, Rev. Sci. Instrum. 72 (2001) 435, https://doi.org/10.1063/1.1309010.
[10] G.S. Lee, et al., Nucl. Fusion 40 (2000) 575, https://doi.org/10.1088/0029-5515/40/3Y/319.
[11] Y.R. Martin, et al., J. Phys.: Conf. Ser. 123 (2008), 012033, https://doi.org/10.1088/1742-6596/123/1/012033.
[12] F. Jaulmes, et al., "Scenarios for physics experiments in the COMPASS Upgrade tokamak", P2b.101 at 48th EPS Conference on Plasma Physics, June 27 – July 1, 2022, Amsterdam, The Netherlands. https://indico.fusenet.eu/event/28/contributions/11/.
[13] F. Jaulmes, et al., Plasma Phys. Control. Fusion 64 (2022), 125001, https://doi.org/10.1088/1361-6587/ac985e.

[14] G. Cunningham, Fusion Eng. Des. 88 (2013) 3238, https://doi.org/10.1016/j.fusengdes.2013.10.001.
[15] J.F. Artaud, et al., Nucl. Fusion 58 (2018), 105001, https://doi.org/10.1088/1741-4326/aad5b1.
[16] O. Février, et al., Nucl. Mater. Energy 27 (2021), 100977, https://doi.org/10.1016/j.nme.2021.100977.
[17] J. Svoboda, et al., Fusion Eng. Des. 168 (2021), 112656, https://doi.org/10.1016/j.fusengdes.2021.112656.
[18] R.J.H. Pearce, et al., Fusion Eng. Des. 82 (2007) 1294, https://doi.org/10.1016/j.fusengdes.2007.07.012.
[19] A. Torres, et al., J. Instrum. 14 (2019), https://doi.org/10.1088/1748-0221/14/09/C09043. C09043.
[20] G. Vayakis, C. Walker, and the ITER International Team and Participant Teams, Rev. Sci. Instrum. 74 (2003) 2409, https://doi.org/10.1063/1.1534388.
[21] M.D. Palma, et al., Fusion Eng. Des. 136 (2018) 1191, https://doi.org/10.1016/j.fusengdes.2018.04.100.
[22] A. Podolnik, et al., "Simulations of Segmented Rail Probes for COMPASS Upgrade", P4.1003 at 46th EPS Conference on Plasma Physics, July 8 to 12, 2019, Milan, Italy. http://ocs.ciemat.es/EPS2019ABS/pdf/P4.1003.pdf.
[23] M. Varavin, et al., Fusion Eng. Des. 146 (2019) 1858, https://doi.org/10.1016/j.fusengdes.2019.03.051.
[24] A. Moroño, E.R. Hodgson, J. Nucl. Mater. 258–263 (1998) 1889, https://doi.org/10.1016/S0022-3115(98)00350-X.
[25] B. Brichard, S. van Ierschot, C. Hendrickx, On the use of photobleaching and thermal annealing to recover the optical transmission in irradiated pure silica fibres, in: 9th European Conference on Radiation and Its Effects on Components and Systems, 2007, pp. 1–4, https://doi.org/10.1109/RADECS.2007.5205465.
[26] R. Scannell, et al., J. Instrum. 12 (2017), https://doi.org/10.1088/1748-0221/12/11/C11010. C11010.
[27] K. Bogar, et al., "The first experimental campaign results of plasmas heated by a new 1 MW neutral beam injector on the COMPASS tokamak", P2b.119 at 48th EPS Conference on Plasma Physics, June 27 – July 1, 2022, Amsterdam, The Netherlands. https://indico.fusenet.eu/event/28/contributions/140/.
[28] J. Varju, et al., "Radiation Shielding for COMPASS-Upgrade", poster #820 at 31st Symposium on Fusion Technology (SOFT2020), 20-25 September 2020, virtual conference.
[29] A. Gusarov, S.K. Hoeffgen, IEEE Trans. Nucl. Sci. 60 (2013) 2037, https://doi.org/10.1109/TNS.2013.2252366.
[30] M. Perry, P. Niewczas, M. Johnston, IEEE Sens. J. 12 (2012) 3248, https://doi.org/10.1109/JSEN.2012.2214030.
[31] A. Morana, et al., IEEE Trans. Nucl. Sci. 63 (2016) 2887, https://doi.org/10.1109/TNS.2016.2618906.
[32] Y. Corre, et al., Fusion Eng. Des. 170 (2021), 112528, https://doi.org/10.1016/j.fusengdes.2021.112528.
[33] E.J. Strait, E.D. Fredrickson, J.-.M. Moret, M. Takechi, Chapter 2: Magnetic Diagnostics, Fusion Sci. Technol. 53 (2) (2008), https://doi.org/10.13182/FST08-A1674, 304.
[34] J. Hlina, J. Reboun, J. Johan, A. Hamacek, Advanced Application Capabilities of Thick Printed Copper Technology, in: 2019 22nd European Microelectronics and Packaging Conference & Exhibition (EMPC), 2019, pp. 1–5, https://doi.org/10.23919/EMPC44848.2019.8951789.
[35] J. Reboun, J. Hlina, R. Soukup, J. Johan, Printed thick copper films for power applications, in: 2018 7th Electronic System-Integration Technology Conference (ESTC), 2018, pp. 1–5, https://doi.org/10.1109/ESTC.2018.8546478.
[36] V. Wei, M. Huang, R. Lai, R. Persons, A comparison study for metalized ceramic substrate technologies: For high power module applications, in: 2014 9th International Microsystems, Packaging, Assembly and Circuits Technology Conference (IMPACT), 2014, pp. 141–145, https://doi.org/10.1109/IMPACT.2014.7048425.
[37] S. Entler, et al., Fusion Eng. Des. 146 (2019) 526, https://doi.org/10.1016/j.fusengdes.2019.01.013.
[38] V. Kindl, et al., Fusion Eng. Des. 171 (2021), 112579, https://doi.org/10.1016/j.fusengdes.2021.112579.
[39] S.G. Lee, J.G. Bak, Rev. Sci. Instrum. 77 (2006) 10E306, https://doi.org/10.1063/1.2227437.
[40] J.-M. Moret, F. Buhlmann, D. Fasel, F. Hofmann, G. Tonetti, Rev. Sci. Instrum. 69 (1998) 2333, https://doi.org/10.1063/1.1148940.
[41] S.P. Gerhardt, et al., Rev. Sci. Instrum. 85 (2014), https://doi.org/10.1063/1.4889781, 11E807.
[42] A. Torres, et al., Fusion Eng. Des. 168 (2021), 112467, https://doi.org/10.1016/j.fusengdes.2021.112467.
[43] B. Gonçalves, et al., ITER prototype fast plant system controller based on ATCA platform, in: 2011 IEEE Nuclear Science Symposium Conference Record, 2011, pp. 171–178, https://doi.org/10.1109/NSSMIC.2011.6154473.
[44] A. Torres, et al., "Data acquisition with real-time numerical integration for COMPASS-U magnetic diagnostics", poster P-1.266 at 32nd Symposium On Fusion Technology (SOFT2022), September 18 –23, 2022, Dubrovnik, Croatia. Also submitted to Fusion Eng. Des.
[45] M. Varavin, et al., "Development status of sub-mm unambiguous interferometer for COMPASS-Upgrade", poster P-2.281 at 32nd Symposium On Fusion Technology (SOFT2022), September 18 –23, 2022, Dubrovnik, Croatia.
[46] P.K. Nesterov, et al., 2020 IEEE Ukrainian Microwave Week (UkrMW), 2020, pp. 862–865. https://doi.org/10.1109/UkrMW49653.2020.9252689.
[47] O. Bogar, et al., Rev. Sci. Instrum. 91 (2020), 013515, https://doi.org/10.1063/1.5099345.
[48] S. Houshmandyar, et al., Rev. Sci. Instrum. 93 (2022), 113514, https://doi.org/10.1063/5.0101790.
[49] A. Huber, et al., 2018 Nucl. Fusion 58 106021. https://doi.org/10.1088/1741-4326/aad481.
[50] K. Kamiya, et al., Fusion Eng. Des. 89 (2014) 3089, https://doi.org/10.1016/j.fusengdes.2014.09.011.
[51] E. Gauthier, et al., Fusion Eng. Des. 82 (2007) 1335, https://doi.org/10.1016/j.fusengdes.2007.06.026.
[52] P. Vondracek, et al., Fusion Eng. Des. 123 (2017) 764, https://doi.org/10.1016/j.fusengdes.2017.05.004.
[53] K. Mikszuta-Michalik, et al., Fusion Eng. Des. 168 (2021), 112421, https://doi.org/10.1016/j.fusengdes.2021.112421.
[54] P. Bohm, et al., Rev. Sci. Instrum. 92 (2021), 083503, https://doi.org/10.1063/5.0043661.
[55] M. Tomes, et al., Rev. Sci. Instrum. 92 (2021), 053532, https://doi.org/10.1063/5.0043786.
[56] M. Ben Yaala, et al., Rev. Sci. Instrum. 92 (2021), 093501, https://doi.org/10.1063/5.0046140.
[57] S. Kajita, et al., Nucl. Fusion 57 (2017), 116061, https://doi.org/10.1088/1741-4326/aa7ef7.
[58] J. Gerardin, et al., Nucl. Mater. Energy 20 (2019), 100568, https://doi.org/10.1016/j.nme.2019.01.002.
[59] A.Q. Kuang, et al., Rev. Sci. Instrum. 89 (2018), 043512, https://doi.org/10.1063/1.5023905.
[60] J. Adamek, et al., Nucl. Fusion 57 (2017), 022010, https://doi.org/10.1088/0029-5515/57/2/022010.
[61] S. Lukes, et al., J. Instrum. 17 (2022) C02007, https://doi.org/10.1088/1748-0221/17/02/C02007.
[62] J. Adamek, et al., Nucl. Fusion 61 (2021), 036023, https://doi.org/10.1088/1741-4326/abd41d.
[63] J. Horacek, et al., Phys. Scr. 96 (2021), 124013, https://doi.org/10.1088/1402-4896/ac1dc9.
[64] F. Jaulmes, et al., J. Fusion Energy 41 (2022) 16, https://doi.org/10.1007/s10894-022-00328-6.
[65] A. Igielski, et al., Nucl. Instr. Meth. A 797 (2015) 210, https://doi.org/10.1016/j.nima.2015.06.044.
[66] Neutral Particle Analyzers. http://www.ioffe.ru/ACPL/npd/npa00.htm.
[67] K. Mitosinkova, et al., PoS 240 (2016) 074, https://doi.org/10.22323/1.240.0074.
[68] K. Bogar, et al., Nucl. Fusion 61 (2021), 036001, https://doi.org/10.1088/1741-4326/abcd75.
[69] J. Caloud, et al., "Conceptual design of Fiber Bragg Grating temperature sensors for heat load measurements in COMPASS-U plasma-facing components", poster #421 at 32nd Symposium On Fusion Technology (SOFT2022), September 18 –23, 2022, Dubrovnik, Croatia. Also submitted to Fusion Eng. Des.
[70] N. Chanet, et al., Fusion Eng. Des. 166 (2021), 112376, https://doi.org/10.1016/j.fusengdes.2021.112376.
[71] M. Tomes, et al., Fusion Eng. Des. 170 (2021), 112498, https://doi.org/10.1016/j.fusengdes.2021.112498.
[72] I. Duran, et al., Fusion Eng. Des. 146 (2019) 2397, https://doi.org/10.1016/j.fusengdes.2019.03.201.
[73] W. Biel, et al., Fusion Eng. Des. 146 (2019) 465, https://doi.org/10.1016/j.fusengdes.2018.12.092.
[74] M. Chernyshova, et al., Nucl. Mater. Energy 33 (2022), 101306, https://doi.org/10.1016/j.nme.2022.101306.
[75] A. Havranek, et al., Fusion Eng. Des. 170 (2021), 112550, https://doi.org/10.1016/j.fusengdes.2021.112550.